

## Dielectric properties and microstructures of $(\text{Ca}_x\text{Sr}_{1-x})\text{ZrO}_3$ ceramics

Yu-De Li, Jian-Ming Chen and Ying-Chieh Lee\*

Department of Materials Engineering National Pingtung University of Technology and Science, Taiwan, R.O.C

The effects of Ca/Sr ratio and the sintering temperature on the properties of  $(\text{Ca}_x\text{Sr}_{1-x})\text{ZrO}_3$  (CSZ) ceramics were investigated in this study. CSZ ceramics were prepared using solid-state reaction process, which were sintered in air at temperatures ranging from 1350 °C to 1450 °C. Their structures were characterized by X-ray Diffraction (XRD), Scanning Electron Microscopy (SEM), and Transmission Electron Microscopy (TEM). The change in Ca/Sr ratio significantly affected the crystalline phase and the dielectric properties of the  $(\text{Ca}_x\text{Sr}_{1-x})\text{ZrO}_3$  ceramics. The secondary phase,  $\text{Ca}_{0.15}\text{Zr}_{0.85}\text{O}_{1.85}$ , was observed and increased correspondingly with the rising of sintering temperatures. In order to understand the effects of secondary phase on the dielectric properties of CSZ ceramics, the  $\text{Ca}_{0.15}\text{Zr}_{0.85}\text{O}_{1.85}$  phase was prepared individually using solid-state method. The  $\text{Ca}_{0.15}\text{Zr}_{0.85}\text{O}_{1.85}$  ceramics sintered at 1500 °C for 2 hours possessed a dielectric constant ( $\epsilon_r$ ) of 21.7, a dielectric loss ( $\tan\delta$ ) of  $49.510^{-4}$  and an Insulation Resistance (IR) of  $2.1 \times 10^{10} \Omega$ . The  $(\text{Ca}_{0.7}\text{Sr}_{0.3})\text{ZrO}_3$  ceramics exhibited the best dielectric properties, with a permittivity of 29, a dielectric loss ( $\tan\delta$ ) of  $2.7 \times 10^{-4}$ , and an Insulation Resistance (IR) of  $2.6 \times 10^{12} \Omega$ .

**Key words:** A. Ceramics, Inorganic Compounds, B. Chemical Synthesis, Microstructure, C. Transmission Electron Microscopy (TEM), X-ray Diffraction, D. Dielectric Properties, Crystal Structure.

### Introduction

The Multilayer Ceramic Capacitors (MLCCs) market has been growing in pace with the development of communication technologies [1].  $\text{CaZrO}_3$  is an interesting material for both mechanical and electrical applications, such as fuel cells, filler, resonator for microwave telecommunication and temperature compensating materials of capacitance in MLCC [2-5].

The dielectric materials with high dielectric constant can effectively decrease the size of resonators, and the dielectric loss must be low enough to achieve prominent frequency selectivity and stability in microwave transmitter components. Moreover, a very small temperature coefficient of resonant frequency is needed to ensure the stability of the microwave components at different working temperatures [6]. Most perovskite-type materials are of interest in capacitors or dielectric resonators microwave applications due to their low dielectric loss and high dielectric constant.  $\text{CaZrO}_3$  is one of such compound, having a dielectric constant around 30, quality factor ( $Q = 1/\tan\delta$ ) of about 3000 at about 5.6 GHz, and a temperature coefficient of resonant frequency ( $\tau_f$ ) of about -26 ppm/°C. However, the  $\text{CaZrO}_3$  ceramic is often sintered at a temperature higher than 1550 °C in order to obtain a

high sample density [1]. It is difficult to apply it in MLCC.

Microwave dielectric properties and microstructures of  $(\text{Ca}_{0.8}\text{Sr}_{0.2})\text{ZrO}_3$  ceramics prepared by the conventional solid-state route have been reported [7]. The values of the dielectric constant ( $\epsilon_r$ ) were 22 ~ 26. The  $Q \times f$  values ranging between 10400 ~ 11500 GHz were obtained when the sintering temperatures were in the range of 1400 ~ 1490 °C. However, the temperature coefficient of the resonant frequency  $\tau_f$  was not sensitive to the sintering temperature.  $\text{CaZrO}_3$  and  $\text{SrZrO}_3$  have the same simple (perovskite) structure like many titanate compounds [8].

As alkaline-earth elements, and the size of  $\text{Sr}^{2+}$  is close to that of  $\text{Ca}^{2+}$ . Therefore, calcium zirconate doped with strontium in any concentration ratio of  $\text{CaZrO}_3$  to  $\text{SrZrO}_3$  is expected to be homogeneous and stable solid solutions as well as perform more interesting characteristics [9].

In this paper, a conventional solid-state reaction procedure was used to synthesize  $(\text{Ca}_x\text{Sr}_{1-x})\text{ZrO}_3$  ceramics. The effects of Ca/Sr ratio and the sintering temperature on the dielectric properties and microstructures of the  $(\text{Ca}_x\text{Sr}_{1-x})\text{ZrO}_3$  ceramics were investigated.

### Experimental Procedure

Samples of  $\text{Ca}_x\text{Sr}_{1-x}\text{ZrO}_3$  ( $0.5 \leq x \leq 0.8$ ) were synthesized using conventional solid-state methods from reagent grade oxide powders  $\text{CaCO}_3$  (Aldrich, 99%),  $\text{SrCO}_3$  (Aldrich, 99.93%), and  $\text{ZrO}_2$  (Aldrich,

\*Corresponding author:  
Tel : +886-8-7703202 ext7556  
Fax: +886-8-7745002  
E-mail: YCLee@mail.npust.edu.tw

99.8%). A mortar and pestle were used to homogenize mixtures of the powders and ethanol, which was added as a medium. The mixtures were then milled with ethanol in a planetary ball mill at 90 rpm for 24 h using yttria-stabilized zirconia balls. The milled powders were dried and calcined at 1150 °C for 2 h in air and then crushed into powders. Next, these powders were mixed with a binder additive (polyvinyl alcohol; PVA) and pressed into disk-shaped specimens. The pellets were sintered in air at temperatures ranging from 1350 °C to 1450 °C for 2 h with heating and cooling rates of 5 °C/min.

Samples of  $\text{Ca}_{0.15}\text{Zr}_{0.85}\text{O}_{1.85}$  ceramics were synthesized using conventional solid-state methods from reagent grade oxide powders  $\text{CaCO}_3$  (Aldrich, 99%), and  $\text{ZrO}_2$  (Aldrich, 99.8%), respectively. A mortar and pestle were used to homogenize mixtures of the powders and ethanol, which was added as a medium. The mixtures were then milled with ethanol in a planetary ball mill at 90 rpm for 24 h using yttria-stabilized zirconia balls. The milled powders were dried and calcined at 1300 °C for 2 h in air, and then crushed into powders. Next, these powders were mixed with a binder additive (polyvinyl alcohol; PVA) and pressed into disk-shaped specimens. The pellets were sintered in air at 1500 °C for 2 h with heating and cooling rates of 5 °C/min.

The crystalline phases of the sintered ceramics were identified by X-ray diffraction pattern analysis (XRD, Bruker D8A, Germany) using  $\text{Cu-K}\alpha$  radiation for  $2\theta$  from 20 to 80. The diffraction spectra were collected at a scan rate of 2.5 °/min. The DIFFRAC plus TOPAS version 3.0 programs were used to determine the lattice parameters. Microstructural observations of the sintered ceramics were performed using a scanning electron microscope (SEM, JEOL, JEL-6400 Japan) coupled with energy-dispersive spectroscopy (EDS). The interior microstructure of the sintered ceramics was investigated by filed-emission TEM (JEOL JEM-2100F, Tokyo, Japan) at an accelerating voltage of 200 kV. The specimens for TEM observations were prepared by slicing, mechanical grinding, and ion milling at 4.0 kV. The bulk density of the sintered pellets was measured using the Archimedes method. Particle sizes were measured using a particle size analyzer (Malvern, Mastersizer 2000, UK). In measuring the dielectric properties, capacitors with various sizes were created by applying copper electrodes to both sides of the pellets, drying the electrodes, and firing them at 900 °C for 10 min in  $\text{N}_2$  atmosphere. The capacitance and dissipation factor were measured at 1 MHz and at 23 °C (HP4278A). The dielectric properties of the samples were measured as a function of temperature, using a HP 4284A LCR meter and a programmable temperature chamber (Agilent Technologies, Palo Alto, CA) interfaced to a PC for automated measurements, and the samples were measured at temperatures ranging from -40 °C to 125 °C. Insulating resistance

measurements were made using a Agilent 4339B meter.

## Results and Discussion

### Density and dielectric property of the $\text{Ca}_{0.15}\text{Zr}_{0.85}\text{O}_{1.85}$ ceramics

To understand the dielectric properties of  $\text{Ca}_{0.15}\text{Zr}_{0.85}\text{O}_{1.85}$  ceramics, which are prepared individually using solid state method. The XRD patterns for the  $\text{Ca}_{0.15}\text{Zr}_{0.85}\text{O}_{1.85}$  ceramics sintered at 1500 °C are shown in Fig. 1(a). All of the XRD peaks can be indexed as a single-phase face center cubic structure. Table 1 lists the permittivity and dielectric loss for the  $\text{Ca}_{0.15}\text{Zr}_{0.85}\text{O}_{1.85}$  ceramics sintered at 1500 °C. The  $\epsilon_r$  value,  $\tan\delta$  and insulation resistance of the  $\text{Ca}_{0.15}\text{Zr}_{0.85}\text{O}_{1.85}$  is approximately 21.7,  $49.5 \times 10^{-4}$  and  $2.11 \times 10^{10}$  W at 1 MHz, respectively. In

**Table 1.** The density and dielectric property of  $\text{Ca}_{0.15}\text{Zr}_{0.85}\text{O}_{1.85}$  ceramics sintered at 1500 °C.

Phase	Density (g/cm <sup>3</sup> )	$\epsilon_r$	$\tan\delta$ ( $\times 10^{-4}$ )	I.R. ( $\Omega$ )
$\text{Ca}_{0.15}\text{Zr}_{0.85}\text{O}_{1.85}$	4.87	21.7	49.5	$2.11 \times 10^{10}$

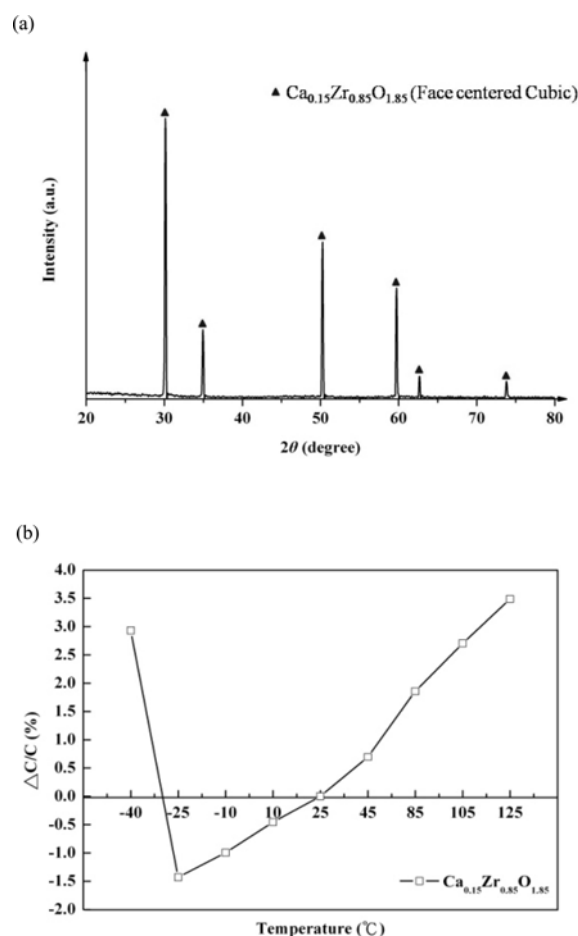


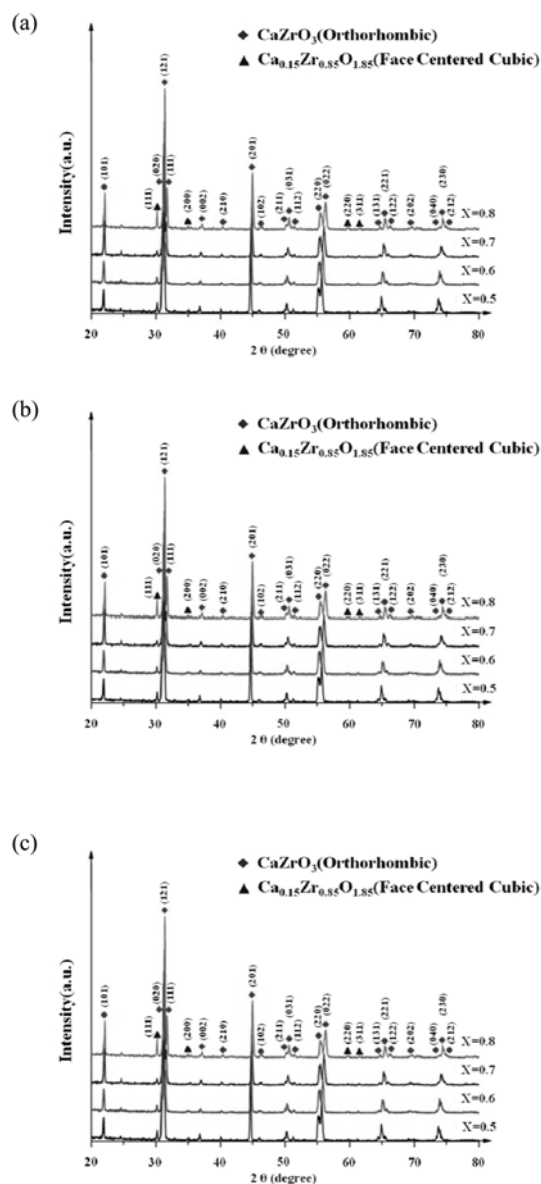
**Fig. 1.** The  $\text{Ca}_{0.15}\text{Zr}_{0.85}\text{O}_{1.85}$  ceramics sintered at 1500 °C, (a) X-ray Diffraction spectra and (b) Temperature Coefficient of Capacitance (TCC).

addition, the temperature coefficient of the capacitance (TCC) of the  $\text{Ca}_{0.15}\text{Zr}_{0.85}\text{O}_{1.85}$  ceramics is shown in Fig. 1(b). The variation of capacitances are from  $-1.5\%$  to  $+3.5\%$  at temperatures ranging from  $-40^\circ\text{C}$  to  $125^\circ\text{C}$ .

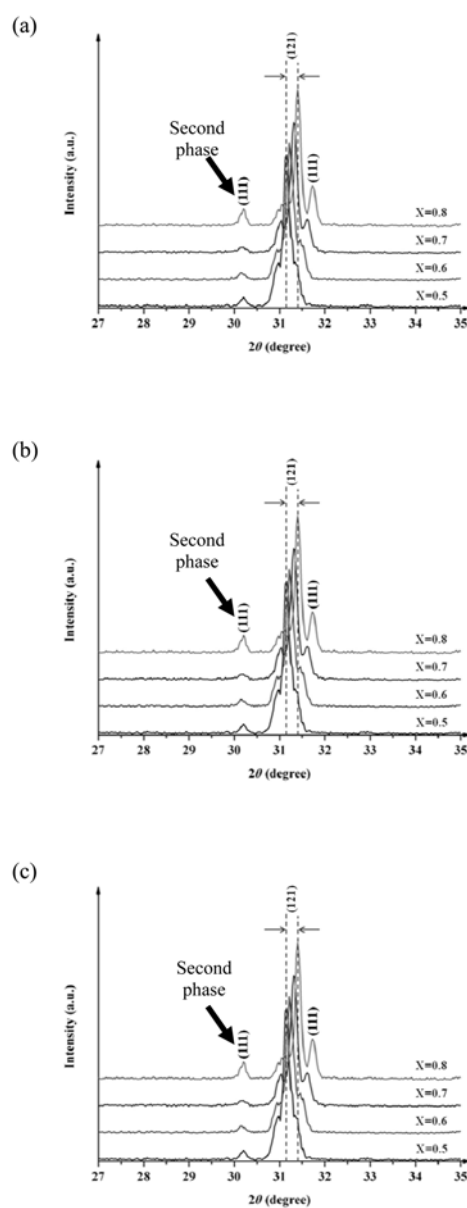
### Phase evolution, density and microstructure in the CSZ ceramics

Fig. 2 shows the XRD patterns of CSZ ceramics sintered at different temperatures and at Ca/Sr ratio. It can be deduced from the XRD patterns that main phase  $\text{CaZrO}_3$  ceramic is obtained after sintering. All peaks excluding the minor secondary phase are indexed for an orthorhombic (*Pcmn*) perovskite structure and are in good agreement with the standard data (ICDD 35-645). There is a secondary phase belonging to  $\text{Ca}_{0.15}\text{Zr}_{0.85}\text{O}_{1.85}$

or  $\text{CaZr}_4\text{O}_9$  ceramics, since both phases have similar XRD peaks. It was clear that the peak strength of secondary phase is enhanced with the rising of sintering temperatures and increasing of Ca/Sr ratio as shown in Fig. 2 and Fig. 3. Further the energy dispersive spectroscopy (EDS) and transmission electron microscopy (TEM) were used to identify the secondary phase. Fig. 3 shows the XRD spectra with  $2\theta$  scale ranging from  $27^\circ$  to  $35^\circ$  only. It can be observed that the (121) peak of  $\text{CaZrO}_3$  phase has shifts to a lower angle when the Ca/Sr ratio was decreased, probably due to substitution of  $\text{Ca}^{2+}$  (ionic radius of  $0.099\text{ nm}$ ) with  $\text{Sr}^{2+}$  (ionic radius of  $0.12\text{ nm}$ ) cation that has a bigger ionic radius. It means that the increase of lattice constants lead to peaks shift to a lower



**Fig. 2.** X-ray diffraction spectra of  $\text{Ca}_x\text{Sr}_{1-x}\text{ZrO}_3$  ceramics with different Ca/Sr ratio, sintered at (a)  $1350^\circ\text{C}$ , (b)  $1400^\circ\text{C}$ , and (c)  $1450^\circ\text{C}$ ,  $2\theta$  ranging from  $20^\circ$  to  $80^\circ$ .



**Fig. 3.** X-ray diffraction spectra of  $\text{Ca}_x\text{Sr}_{1-x}\text{ZrO}_3$  ceramics with different Ca/Sr ratio sintered at (a)  $1350^\circ\text{C}$ , (b)  $1400^\circ\text{C}$ , and (c)  $1450^\circ\text{C}$ ,  $2\theta$  ranging from  $27^\circ$  to  $35^\circ$ .

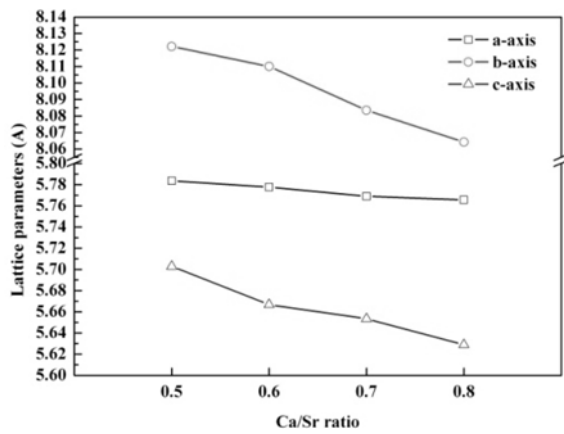


**Fig. 4.** The lattice parameters of  $\text{Ca}_x\text{Sr}_{1-x}\text{ZrO}_3$  ceramics sintered at 1400 °C for different Ca/Sr ratio.

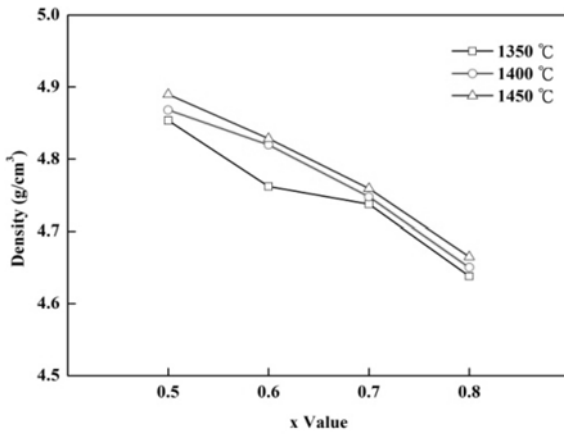


**Fig. 5.** Density of  $\text{Ca}_x\text{Sr}_{1-x}\text{ZrO}_3$  ceramics as a function of sintering temperature and Ca/Sr ratio.

angle [10, 11]. Fig. 4 shows the variation between the CSZ lattice parameters sintered at 1400 °C with different Ca/Sr ratio. An increase in Ca/Sr ratio leads to a decrease in b and c, which may be attributed to the ionic radius of  $\text{Ca}^{2+}$  being smaller than that of  $\text{Sr}^{2+}$ . The ionic radius of  $\text{Ca}^{2+}$  and  $\text{Sr}^{2+}$  are 0.134 nm and 0.144 nm, respectively [12]. This result was consistent with XRD peaks being shifted as shown in Fig. 3.

CSZ ceramics with different Ca/Sr ratio were sintered in air at temperatures ranging from 1350 ° to 1450 °C for 2 h. The average particle size of the starting powder was  $0.8 \pm 0.1$  μm in all experiments. Fig. 5 shows the bulk density of the CSZ ceramics as a function of the Ca/Sr ratio and sintering temperatures. With an increasing Ca/Sr ratio, the bulk density of the CSZ ceramics gradually decreases significantly. This is attributed to the density of the  $\text{CaZrO}_3$  (4.62 g/cm<sup>3</sup>) which is smaller than  $\text{SrZrO}_3$  (5.445 g/cm<sup>3</sup>) [12, 13]. Moreover, with increasing sintering temperatures, the bulk density of the CSZ ceramics gradually increases correspondingly.

The SEM micrographs of the CSZ ceramics sintered at 1400 °C with different Ca/Sr ratio are shown in Fig.

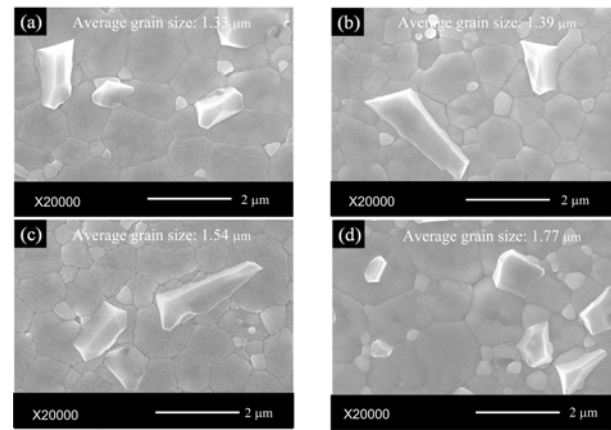


**Fig. 6.** Scanning electron micrography images of  $\text{Ca}_x\text{Sr}_{1-x}\text{ZrO}_3$  ceramics with different Ca/Sr ratio (a)  $x = 5$ , (b)  $x = 6$ , (c)  $x = 7$  and (d)  $x = 8$ , all sintered at 1400 °C for 2 h.

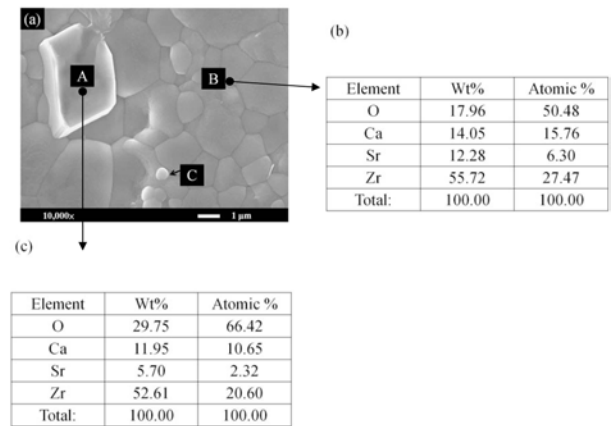


**Fig. 7.** SEM images of  $\text{Ca}_{0.7}\text{Sr}_{0.3}\text{ZrO}_3$  ceramics sintered at 1400 °C showing (a) SEM images, (b) the EDS of matrix grains, and (c) the EDS of secondary phase grains.

6(a)-(d), respectively. An obvious difference among the images is the grain size which depends on the Ca/Sr ratio. The grain size in the specimens with Ca/Sr ratio at 5/5, 6/4, 7/3 and 8/2 was 1.33, 1.39, 1.54 and 1.77 μm, respectively.

The grain size in the CSZ ceramics decreases significantly as the Ca/Sr ratio decreased. The lattice strain was created when Sr was substituted to Ca-site in the lattice, since  $\text{Ca}^{2+}$  and  $\text{Sr}^{2+}$  radius are 0.099 nm and 0.12 nm, respectively. Too much lattice strain will lead to Sr ions being precipitated into grain boundary, which is thermodynamically more stable. Grain boundaries would be pinned by these defects, inhibiting grain growth, thereby, resulting in relatively small grains. [14-16] Moreover,  $\text{CaZrO}_3$  melting temperature ( $T_m = 2340$  °C) is indeed lower than that of  $\text{SrZrO}_3$  ( $T_m = 2750$  °C), [17, 18] thus, when the Ca/Sr ratio is increased, the grain size is grown. It is clear that the rectangle-like grains such as secondary phases are observed in whole samples, and the secondary phases are enhanced with an increasing Ca/Sr ratio. This result

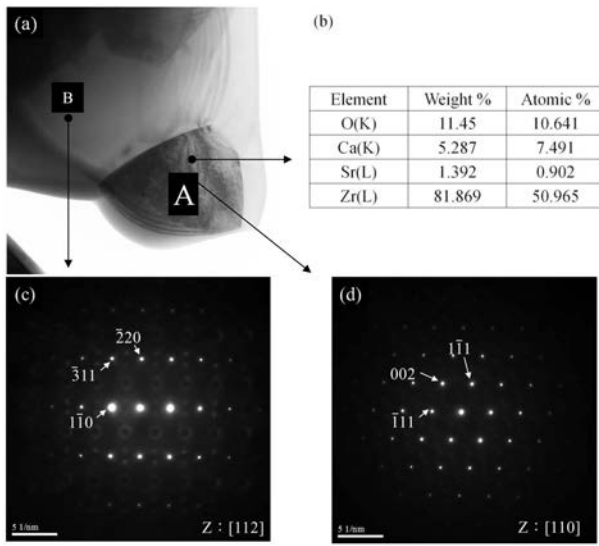


**Fig. 8.** HRTEM images of  $\text{Ca}_{0.7}\text{Sr}_{0.3}\text{ZrO}_3$  ceramics sintered at  $1400^\circ\text{C}$  showing (a) TEM images, (b) the EDX of secondary phase grains, (c) and (d) the SAD of  $\text{Ca}_{0.15}\text{Zr}_{0.85}\text{O}_{1.85}$  grains.

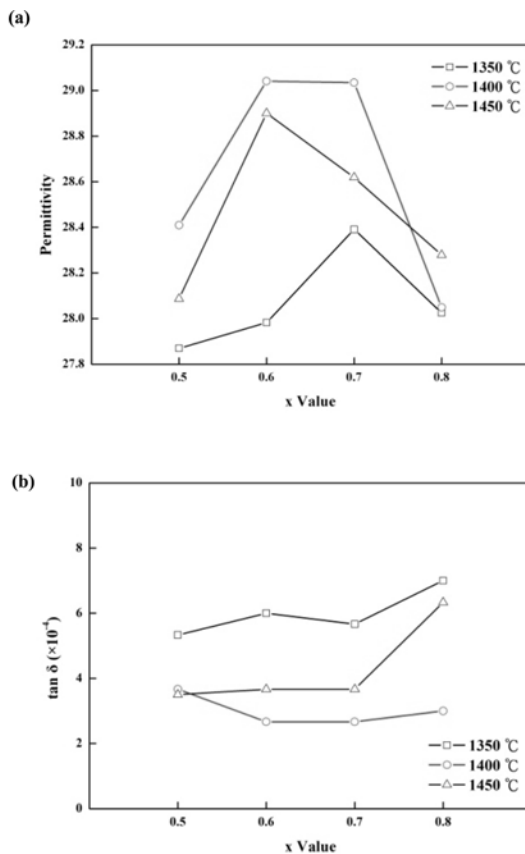


**Fig. 9.** The dielectric properties of  $\text{Ca}_x\text{Sr}_{1-x}\text{ZrO}_3$  ceramics as a function of sintering temperature and Ca/Sr ratio: (a) dielectric constants ( $\epsilon_r$ ) and (b) dielectric loss ( $\tan\delta$ ).

is consistent with XRD analysis as shown in Fig. 3. The energy-dispersive spectroscopy (EDS) of the  $\text{Ca}_{0.7}\text{Sr}_{0.3}\text{ZrO}_3$  specimens sintered at  $1400^\circ\text{C}$  is shown in Fig. 7. The EDS analysis indicates that the matrix

grains “B” belonged to the CSZ phase, while the rectangle-like grains “A” belonged to the  $\text{Ca}_{0.15}\text{Zr}_{0.85}\text{O}_{1.85}$  phase as shown in Fig. 7(b) and 7(c).

To study the secondary phase, TEM was used to observe the microstructure in  $\text{Ca}_{0.7}\text{Sr}_{0.3}\text{ZrO}_3$  ceramics sintered at  $1400^\circ\text{C}$ , as shown in Fig. 8. The electron diffraction patterns of the CSZ ceramics are shown in Fig. 8(c) and 8(d). The matrix grains (B) and secondary phase grains (A) were identified as CSZ and  $\text{Ca}_{0.15}\text{Zr}_{0.85}\text{O}_{1.85}$  phase, respectively, according to the electron diffraction patterns.

### Dielectric properties of the CSZ ceramics

The  $\text{CaZrO}_3$  material exhibits a relatively high permittivity (25-30), low dielectric losses ( $< 10^{-4}$ ), a high insulating resistivity ( $> 10^{12} \Omega$ ) and a temperature coefficient of resonant frequency ( $\tau_f$ )  $40 \text{ ppm}/^\circ\text{C}$ . and also for its inertia to the reductive atmosphere [19, 20]. The  $(\text{Ca}_{0.8}\text{Sr}_{0.2})\text{ZrO}_3$  ceramics sintered at  $1480^\circ\text{C}$  for 2-12 h possessed a dielectric constant ( $\epsilon_r$ ) of 23.6-27.9, a quality factor ( $Qxf$ ) of 2,160-21,460 GHz and a temperature coefficient of resonant frequency ( $\tau_f$ ) from -14 to  $13.6 \text{ ppm}/^\circ\text{C}$ . [6]

Fig. 9(a) shows the variation of the permittivity and dielectric loss recorded for the  $(\text{Ca}_x\text{Sr}_{1-x})\text{ZrO}_3$  ceramics sintered ranging from  $1350^\circ\text{C}$  to  $1450^\circ\text{C}$  with respect to their  $x$  value. By increasing the  $x$  value, the dielectric constant of CSZ ceramics sintered at  $1400^\circ\text{C}$  initially increases at  $x = 0.6$ , then decreases to a minimum at  $x = 0.8$ . For CSZ ceramics sintered at  $1450^\circ\text{C}$ , by increasing the  $x$  value, the dielectric constant initially increases significantly at  $x = 0.6$ , then decreases gradually to  $x = 0.8$ . As we known, the  $\text{Ca}_{0.15}\text{Zr}_{0.85}\text{O}_{1.85}$  is the secondary phase which has a dielectric constant ( $\epsilon_r$ ) of 21.7. It is therefore believed that lower permittivity is contributed to by the existence of secondary phases. According to J. C. Maxwell's equation: [21]

If  $\sim 20 \text{ vol.}\%$   $\text{Ca}_{0.15}\text{Zr}_{0.85}\text{O}_{1.85}$  rectangle-like phase is occupied in host ceramic (Fig. 7(a)), the dielectric constant of CSZ ceramic is calculated as listed below:

$$\epsilon_m = \epsilon_2 \left\{ 1 + \frac{3V_f(\epsilon_1 - \epsilon_2)}{\epsilon_1 + 2\epsilon_2 - V_f(\epsilon_1 - \epsilon_2)} \right\} \quad (1)$$

where  $V_f$  is the volume fraction occupied by the dispersed phases,  $\epsilon_1$  and  $\epsilon_2$  are the permittivity of  $\text{Ca}_{0.15}\text{Zr}_{0.85}\text{O}_{1.85}$  and pure CSZ ceramic, respectively;  $\epsilon_m$  is permittivity of mixtures (CSZ). The dielectric constant of the CSZ ceramics are estimated from the values of pure  $\text{Ca}_{0.15}\text{Zr}_{0.85}\text{O}_{1.85}$  ceramics (21.7) and  $(\text{Ca}_{0.7}\text{Sr}_{0.3})\text{ZrO}_3$  ceramics ( $\sim 30$ ). The estimated dielectric constants for  $(\text{Ca}_{0.7}\text{Sr}_{0.3})\text{ZrO}_3$  ceramics with  $\text{Ca}_{0.15}\text{Zr}_{0.85}\text{O}_{1.85}$  secondary phase is  $\sim 29.2$ . In addition, the CSZ ceramics sintered at  $1350^\circ\text{C}$ , has lower dielectric constant as compared with  $1400^\circ\text{C}$  and  $1450^\circ\text{C}$ . This is attributed to insufficiency of densification.

Fig. 9(b) shows the dielectric loss of the CSZ

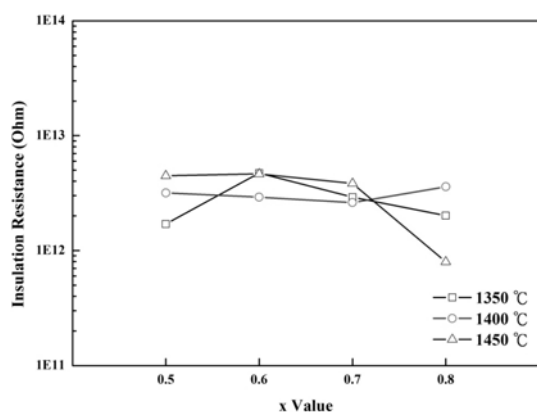


**Fig. 10.** The insulation resistance of  $\text{Ca}_x\text{Sr}_{(1-x)}\text{ZrO}_3$  ceramics as a function of sintering temperature and Ca/Sr ratio.

ceramics as a function of the sintering temperatures and  $x$  values. When sintering temperature is at 1400 °C, a lower dielectric loss is obtained. It may be attributed to the formation of more  $\text{Ca}_{0.15}\text{Zr}_{0.85}\text{O}_{1.85}$  secondary phases with the sintering temperature increasing from 1400 °C to 1450 °C, as illustrated in Fig. 3, because the  $\text{Ca}_{0.15}\text{Zr}_{0.85}\text{O}_{1.85}$  phase has a higher dielectric loss ( $49.5 \times 10^{-4}$ ) and contributes to the  $\tan\delta$  value of its host material. In addition, the dielectric loss of the CSZ ceramics is enhanced at lower sintering temperatures (1350 °C), this is due to the insufficient densification of CSZ ceramics. There are many factors affected on the microwave dielectric loss ( $1/Q$ ) of ceramics, it can be divided into two categories, that is, intrinsic loss and extrinsic loss [22]. Intrinsic losses are mainly caused by lattice vibration modes, while extrinsic losses are dominated by second phase, oxygen vacancies, grain sizes, and densification or porosity [23].

Fig. 10 shows the insulation resistance of the CSZ ceramics as a function of the sintering temperatures and  $x$  values. Insulation resistance of all samples can reach  $>10^{12} \Omega$ , except  $(\text{Ca}_{0.8}\text{Sr}_{0.2})\text{ZrO}_3$  ceramics sintered at 1450 °C. Because the  $\text{Ca}_{0.15}\text{Zr}_{0.85}\text{O}_{1.85}$  phase has a lower insulation resistance ( $2.1 \times 10^{10} \Omega$ ) and reduce to the IR value of its host material.

## Conclusions

$(\text{Ca}_x\text{Sr}_{(1-x)})\text{ZrO}_3$  ceramics were prepared using a solid-state reaction method, which were sintered in air at temperatures ranging from 1350 °C to 1450 °C. The different Ca/Sr ratio significantly affected the crystalline phases and the microwave dielectric properties of the  $(\text{Ca}_x\text{Sr}_{(1-x)})\text{ZrO}_3$  ceramics. The grain size in the CSZ ceramics decreases significantly as the Ca/Sr ratio decreased. The formation of a secondary phase ( $\text{Ca}_{0.15}\text{Zr}_{0.85}\text{O}_{1.85}$ ) could be increased by increasing the sintering temperature. The dielectric properties of  $\text{Ca}_{0.15}\text{Zr}_{0.85}\text{O}_{1.85}$  phase was prepared individually using solid-state method. The  $\text{Ca}_{0.15}\text{Zr}_{0.85}\text{O}_{1.85}$  ceramics sintered at

1500 °C for 2 hours possessed a dielectric constant ( $\epsilon_r$ ) of 21.7, a dielectric loss ( $\tan\delta$ ) of  $49.5 \times 10^{-4}$  and an Insulation Resistance (IR) of  $2.1 \times 10^{10} \Omega$ . When the  $(\text{Ca}_{0.7}\text{Sr}_{0.3})\text{ZrO}_3$  ceramic was sintered at a temperature of 1400 °C, which had the best microwave dielectric properties, with a permittivity of 29 and a dielectric loss ( $\tan\delta$ ) of  $2.7 \times 10^{-4}$  and an Insulation Resistance (IR) of  $2.6 \times 10^{12} \Omega$ .

## References

1. M. Pollet, S. Marinell, Mater. Sci. Eng., A362 (2003) 167-173.
2. K. Kiyoshi, Y. Shu, I. Yoshiaki, Solid State Ionics, 108 (1998) 355-359.
3. Y. Suzuki, P.E.D. Morgan, T. Ohji, J. Am. Ceram. Soc., 83 (2000) 2091-2096.
4. S.K. Lim, H.Y. Lee, J.C. Kim, C. An, IEEE Microw. Guided Wave Lett., 9 (1999) 143-144.
5. Woo-Jin Lee, Akihiro Wakahara, Bok-Hee Kim, Ceram. Intl., 31 (2005) 521-524.
6. Weina Chen, Huiqing Fan, Changbai Long, J Mater Sci, Mater. Electron, 25 (2014) 1505-1511.
7. Cheng-Hsing Hsu, Chia-Hao Chang, Wen-Shiush Chen, Jenn-Sen Lin and Chun-Hung Lai, Mater. Sci. Forum, 787 (2014) 338-341.
8. H. Stetson, B. Schwartz, J. Am. Ceram. Soc., 44 (1961) 420-421.
9. Changhong Chen, Dexiu Huang, Weiguang Zhu, Xi Yao, Appl. Surf. Sci., 252 (2006) 7585-7589.
10. S. Hesarak, S. Farhangdoust, K. Ahmadi, R. Nemati and M. Khorami, J. Austr. Ceram. Soc., 48 [2] (2012) 166-172.
11. Yi-Seul Kim, Sung-Woo Choi, Jeong-Hwan Park, Eun Bok, Byung-Ki Kim and Seong-Hyeon Hong, J. Solid State Sci. & Tech., 2 [2] (2013)R3021-R3025.
12. R.D. Shannon, Acta Crystallogr., A32 (1976) 751-767.
13. Maik Lang, Fuxiang Zhang, Weixing Li, Daniel Severin, Markus Bender, Siegfried Klaumunzer, Christina Trautmann, Rodney C Ewing, Nuclear Instruments and Methods in Physics Research B, 286 (2012) 271-276.
14. Chunsheng Shi and Masahiko Morinaga, J. Comput. Chem., 27 [6] (2006) 7118-7120.
15. Yi, J. Y.; Lee, J. K. & Hong, K. S., J. Am.Ceram. Soc., 85 (2002) 3004-3010.
16. Lewis, G. V.; Catlow, R. A. & Casselton, J. Am. Ceram. Soc., 68 (1985) 555-558.
17. Yeon Soo Sung and Myong Ho Kim, Ferroelectrics, 13 (2010) 217-230.
18. Zushu Li, William Edward Lee, and Shaowei Zhang, J. Am. Ceram. Soc., 90 [2] (2007) 364-368.
19. Michael Pollet, Sylvain Marinell, Francois Roulland, J. Eur. Ceram. Soc., 25 (2005) 2773-2777.
20. Woo-Jin Lee, Akihiro Wakahara, Bok-Hee Kim, Ceram. Intl., 31 (2005) 521-524.
21. A. J. Moulson and J. M. Herbert, Electroceramics, Materials Properties Applications, London, 79 (1990) 79-82.
22. C.L. Huang, M.-H. Weng and H.-L. Chen, Mater. Chem. Phys., 71 (2001) 17-22.
23. Kwan Soo Kim, Sang Heung Shim, Shin Kim and Sang Ok Yoon, Journal of Ceramic Processing Research, 11 [1] (2010) 47-51.